Polym. Bull. (2010) 64:171–183
DOI 10.1007/s00289-009-0155-7

Preparation and characterization of poly(acrylic acid)/pillared clay superabsorbent composite

Zehra Bekçi Molu · Yoldaş Seki · K. Yurdakoç

Received: 10 March 2009 / Revised: 17 June 2009 / Accepted: 6 September 2009 /
Published online: 12 September 2009

Abstract Pillared clay-based superabsorbents (PILC-SA) were synthesized by using Al pillared-montmorillonite K10 and KSF via graft copolymerization reaction of acrylic acid (AA). Swelling behavior of pillared clay-based superabsorbent films in distilled water and at different pH values were investigated at room temperature. It was also obtained that Al-KSF and Al-K10 based superabsorbents were pH dependent and showed a reversible swelling behavior. Water absorbency of Al-KSF based superabsorbent was higher than that of Al-K10 based one. SEM, FTIR, and XRD analysis were conducted for further characterization of the PILC-SA. FTIR analyses lead to ester formation between PILC and SA. XRD revealed the basal spacing of the pillared clays before and after in situ incorporation indicating that the morphology of the superabsorbent was exfoliated and the layers of clay dispersed on the composite.

Keywords Hydrogel · Superabsorbent composite · Swelling · pH sensitivity · Pillared clay

Introduction

Superabsorbent hydrogels are a type of loosely crosslinked hydrophilic polymer that can swell, absorb and retain a large volume of water or other biological fluid. Superabsorbents may have found many application fields owing to the water absorbing characteristics. Some of their applications include novel moisture sensors, fire protection materials, hygienic products, horticulture, gel actuators, drug-delivery systems, as well as water blocking tapes and coal dewatering [1–9].

Z. B. Molu · Y. Seki · K. Yurdakoç (✉)
Department of Chemistry, Faculty of Arts and Sciences, Dokuz Eylül University, Buca, 35160 İzmir, Turkey
e-mail: k.yurdakoc@deu.edu.tr

Recently, research on the use of superabsorbents as water managing materials for the renewal of arid and desert environment has attracted great attention, and encouraging results have been observed as they can reduce irrigation water consumption, improve fertilizer retention in soil, lower the death rate of plants, and increase plant growth rate [10]. Additionally, superabsorbents have negative features in some application fields because of high production cost and low gel strength. To overcome these negative points, inorganic fillers can be used as low cost material and improve the strength properties in the polymer matrixes. In the superabsorbent field, much attention has been paid to layered silicate recently for the preparation of superabsorbent composites because of developing mechanical and materials properties of superabsorbent. Clays, such as kaolin [11], montmorillonite [12–14], attapulgite [15, 16], mica [17], bentonite and sercite [18], hydrotalcite [19] have all been used for the preparation of superabsorbent composites. Pillared clays are modified clays that protect the layered silicate structure.

In the present study, pillared clays were used as inorganic materials for developing the properties of superabsorbent hydrogels. It was reported that the intercalation of certain metal oxides on 2:1 clay minerals significantly led to an increase in the sorption capacity [20]. High temperature calcination of intercalated clays results in 'pillared' materials, where the polyhydroxo cationic species are irreversibly fixed to the layers. Al-pillared montmorillonite KSF (Al-KSF) and Al-pillared montmorillonite K10 (Al-K10) were pillared clays that used as inorganic fillers. The introduction of pillars (Keggien ion), besides increasing the material's resistance and stability, provides porosity, a greater surface area, access to acid areas existing in natural clay, and the presence of potentially active species for a specific reaction [21, 22]. The increase in interfacial interactions via hydrogen bonds or covalent bonds between the organic and inorganic phases will result in superior properties compared to classical composites [23]. For that reason, the performance of the inorganic fillers on the properties of the superabsorbents was compared each other in detail. Zhang et al. examined the intercalation of sodium methyl allyl sulfonate (SMAS) into Hydrotalcite (HT) promotes the layers of HT more hydrophilic, enabling them to be exfoliated by acrylate molecules and to prepare the exfoliated poly(sodium acrylate) (PSA)/HT (PSA/HT) nanocomposite superabsorbents and supported the exfoliation of layers by XRD analysis [24]. In this study, XRD analysis revealed that the layers of Montmorillonite K10 and KSF were exfoliated by polymerization. Additionally, the synthesis of pillared clays containing acrylic-based superabsorbent hydrogel composites and the characterization performed by XRD, FT-IR, and SEM were represented.

Materials and methods

Chemicals and reagents

Acrylic acid (AA) and the crosslinker *N*,*N*′-methylene-bisacrylamide (MBA) purchased from Fluka were used without further purification. Ammonium persulfate

(APS), sodium metabisulfite (SMBS), and potassium hydroxide (KOH) (all from Merck) were used as received.

KSF montmorillonite (KSF) and K10 montmorillonite (K10) supplied from Fluka Company were utilized as precursor material of pillared clays. Chemical composition of KSF Montmorillonite is 55.0% SiO_2, 18.0% Al_2O_3, 4.0% Fe_2O_3, 3.0% MgO, 3.0% CaO, <0.5% Na_2O, 1.5% K_2O, 5.0% sulfate, and 10.0% loss on ignition. KSF has a surface area of 20–40 m^2/g. Chemical composition of K10 is 69.0% SiO_2, 14.0% Al_2O_3, 4.5% Fe_2O_3, and 2.0% MgO, 1.5% CaO, <1.5% Na_2O, 1.5% K_2O, and 7.0% ignition loss. K10 has a surface area of 197 m^2/g.

Synthesis of pillared clays

The $AlCl_3 \cdot 6H_2O$ and NaOH purchased from Merck were used to prepare the pillaring solution for the synthesis of aluminum pillared clay.

The pillaring solution was prepared by titrating aqueous 0.1 M NaOH with aqueous 0.1 M $AlCl_3 \cdot 6H_2O$ until the OH/Al ratio was equal to 2.0. At this hydrolysis ratio, Al_{13} is a major species in solution. The pillaring solution was aged for 2 h at 60 °C and then kept overnight at 30 °C. After aging, the resulting solution reacted with a proper amount of aqueous suspension of KSF and K10 clay, keeping an Al/clay ratio of 10 mmol g^{-1}. The slurries were maintained at 60 °C for 2 h followed by an aging period of 7 days at room temperature, then washed by centrifugation and dialysis till the absence of chloride and oven dried at 80 °C for 18 h and calcined at 250 °C for 2 h.

Synthesis of superabsorbent composite

Acrylic acid (20 g) was neutralized with potassium hydroxide solution (12.1 g KOH + 10.0 g H_2O). Then crosslinker (MBA) solution (0.013 g MBA + 3.0 g H_2O) was added to the monomer solution. The mixture was poured into a 600-mL beaker, which was equipped with a magnetic stirrer and thermometer. 0.05 g of Al-KSF and Al-K10 were added to stirring solutions and stirring was continued for 5 min until homogeny mixtures were obtained. To start polymerization reaction, the APS solution (0.05 g APS + 1.5 g H_2O) and the SMBS solution (0.063 g SMBS + 2 g H_2O) were added to the mixture to accelerate the polymeric reaction. The temperature of mixture was increase rapidly to almost 100 °C within a few minutes. Prior to hardening the products, the mixtures were pour into the Petri dish to obtain thin films. Samples were dried in a vacuum oven at 70 °C for 24 h and then a few amount of water was dropped to film and after 1 h, the film was removed from Petri dish and cut into an appropriate size ($\sim$1 cm $\times$ 1 cm). After all, samples were dried again.

Swelling measurements

Water absorbency measurement was performed weighing the initial mass of composite (m_0) and mass determined at time t (m_t) of gel that was immersed in the

distilled water at room temperature. Swollen samples were then separated from unabsorbed water by using tissue paper until reaching the swelling equilibrium. The percent of swelling values were calculated by the Eq. 1 [25]. Data points are means of three measurements.

$$\%\text{Swelling} = 100\left[\frac{(m_t - m_0)}{m_0}\right] \quad (1)$$

BET (Brunauer, Emmett, Teller) analysis

BET surface areas (S_{BET}) of Al-KSF and Al-K10 were obtained from N_2 adsorption–desorption isotherms at 77 K, measured on SORPTOMATIC 1990 after a degassing under vacuum for 3 h at 150 °C by using MILES-200 Advanced Data Processing Sorption Software Version 3.00. Al-KSF has a surface area of 76.62 m^2/g. Total pore volume (V_{total}) and average pore diameter (l_p) of Al-KSF were 0.123 mL/g and 6.402 nm, respectively. K10 had a surface area of 197 m^2/g. By pillaring with Al-polyoxycation, the BET surface area was increased, the value of surface area was 234.52 m^2/g. Total pore volume (V_{total}) and average pore diameter (l_p) of Al-K10 were 0.364 mL/g and 6.208 nm, respectively. It was concluded that pillared clays had much greater surface areas than K10 and KSF. It was beneficial for forming crosslink points.

Morphology of superabsorbents

SEM micrographs and elemental analysis were performed by a scanning electron microscope (SEM; Jeol JSM 60) operating at the accelerating voltage of 20 kV. The film of composite samples was dried before gold sputter-coated for SEM analysis.

Fourier transforms infrared spectroscopy (FTIR) analysis

The IR spectra of the superabsorbent composite were recorded on a FTIR (Perkin Elmer Spectrum BX-II) using ATR probe at ambient conditions for film of composite. For analysis of pillared clays, KBr pellets were prepared. Infrared spectra were carried out in the region of 4,000–400 cm^{-1}.

XRD analysis

X-ray powder diffraction patterns were obtained by Rigaku Dmax 2200/PC model instrument with Cu K_α radiation (40 kV, 40 mA). Clays, pillared clays, and superabsorbent samples for X-ray diffraction (XRD) measurement were processed to powder form and film form for pillared clays and superabsorbents, respectively. The space of the layer is calculated by this formula $2d\sin\theta = n\lambda$ [26]. XRD reveals the basal spacing of the pillared clays before and after in situ incorporation indicating the morphology of the superabsorbent (exfoliated, intercalated or only dispersed).

Results and discussion

Swelling capacity

Figure 1 shows swelling values of the Al-KSF and Al-K10 based superabsorbents in distilled water. Al-KSF and Al-K10 based superabsorbents (Al-KSF-SA and Al-K10-SA) reached equilibrium within 100 min. The percentages of equilibrium swelling values were at about 7900 for Al-KSF-SA and at about 5700 for Al-K10-SA. As shown from Fig. 1, Al-KSF based composites had greater equilibrium swelling values than Al-K10 based superabsorbent. This might be due to network of superabsorbent. In addition, crosslink density and elasticity of polymer network might affect the water absorption of hydrogels. Seki et al. determined that water absorbency values for iron rich smectite superabsorbent were about 230 times the weight of the superabsorbent hydrogel under normal atmospheric conditions [27]. The value which is obtained in this study can be considered as low values. It is probable that pillared clays may function as a crosslinking agent. If it is possible, carboxylate groups of the polyacrylate chains may react with OH groups of pillared clays. From Fig. 1, it can be inferred that more crosslink points may occur between Al-K10 pillared clay and SA. Al-polyoxycation and the OH groups of the pillared clay act as crosslinking points. The amount of pillaring agent used in pillaring is same. Also, same procedures were applied in the preparation of pillared clay-based superabsorbents (PILC-SA) and the single change was precursor clay. Additionally, K10 has more active points by pillaring and the surface area was greater than the Al-KSF. Because of the formation of additional network, the remaining space for water to enter reduces.

pH sensitivity of the superabsorbents

pH sensitivity of superabsorbent was also evaluated by immersing films in different buffer solutions. Figure 2 was plotted so as to determine the effect of pH on equilibrium swelling. As observed from Fig. 2, pH affected swelling values of

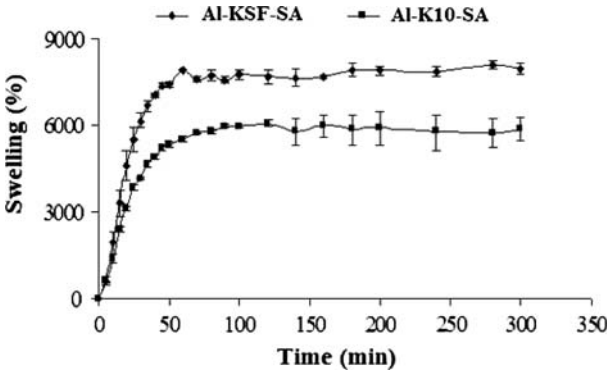

Fig. 1 Swelling kinetics of superabsorbents composite in distilled water

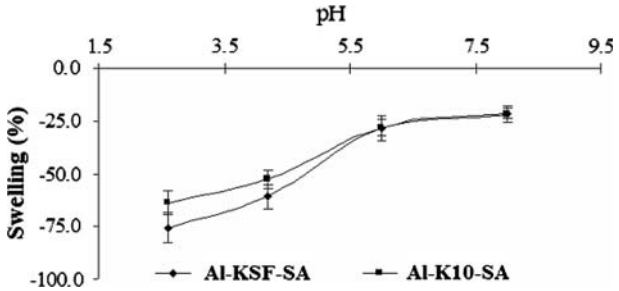

Fig. 2 Effect of pH on the swelling equilibrium of superabsorbents

superabsorbent and deswelling occurred. Equilibrium deswelling values were decreased with increasing of pH values until pH of 5.5. Beyond the pH value of 5.5, deswelling values were almost similar to each other. At low pH values, it was seen that Al-KSF based superabsorbent had slightly greater deswelling values than Al-K10 based superabsorbent. As a result, it had been reached that the swelling behavior of Al-KSF and Al-K10 based superabsorbent films seem to be pH dependent.

Higher hydration and distension could increase the interaction between polymeric network and clay, which increases crosslink density of obtained superabsorbent composite, and then decreases the equilibrium water absorbency. For example, Na^{+}-montmorillonite has the highest hydration and distension among the clays selected, and then the lowest equilibrium water absorbency of corresponding superabsorbent composites [28].

Swelling reversibility of Al-KSF and Al-K10 based superabsorbents

The swelling reversibility of superabsorbents was alternately conducted at pH = 1.2 and 7.8. After superabsorbents were equilibrated at pH = 7.8, and then alternated between solutions at pH = 1.2 and pH = 7.8, respectively. Superabsorbents were equilibrated at pH = 7.8, then the samples were immersed in pH = 1.2 for about 180 min. It was understood from Fig. 3 that a shrinking was measured at about 80–90%. Then the films put into pH = 7.8 for 180 min and approximately 55–60% swelling was determined. When the pH values were varied repeatedly, Al-KSF and Al-K10 based superabsorbents exhibited a reversible swelling behavior with relatively fast response. It can be added that reversible swell–shrink properties of Al-KSF and Al-K10 based superabsorbents would be beneficial characteristics for pH sensitive systems with controllable swelling ability. Al-KSF and Al-K10 based superabsorbents indicated similar behaviors to acidic and basic medium. In basic conditions, the polymeric chain was expanded because of –COO– groups of chain. The negative groups of polymeric chain repelled each other. As a result of repulsion, the superabsorbent composite swelled. And also in acidic conditions, the shrinkage was occurred because of –COOH groups of polymeric network. No repulsion was observed. The polymer responded both acidic and basic media rapidly.

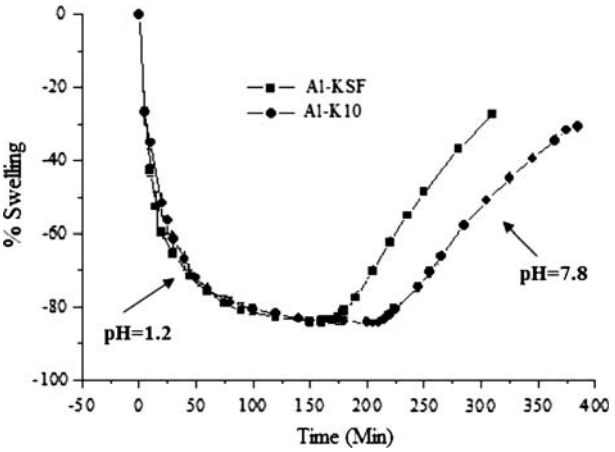

Fig. 3 pH-dependent reversible swelling behavior of superabsorbents (Superabsorbents equilibrated at pH = 7.8, then alternated between solutions at pH = 1.2 and pH = 7.8)

SEM images

SEM micrographs of Al-K10, Al-K10-SA and Al-KSF, Al-KSF-SA were shown in Figs. 4a, b, 5a, b, respectively. Water absorbency capacity of superabsorbents might be related to the porosity of clays as used as fillers and level of crosslinking. As seen in the micrograph of Al-K10, it was clear that the pores were observed on the surface of the clay structure. After graft polymerization with Al-K10, Al-K10 was dispersed homogenous on hydrogel. From SEM images of Al-KSF and Al-KSF-SA, it was deduced from the micrograph of Al-KSF based composite that the homogenous dispersion of pillared clay was lower than Al-K10 based composite and the pores were not observed clearly from the morphology of Al-KSF. In other words, it was expected that the water absorbency of Al-KSF based composite was higher than Al-K10-SA.

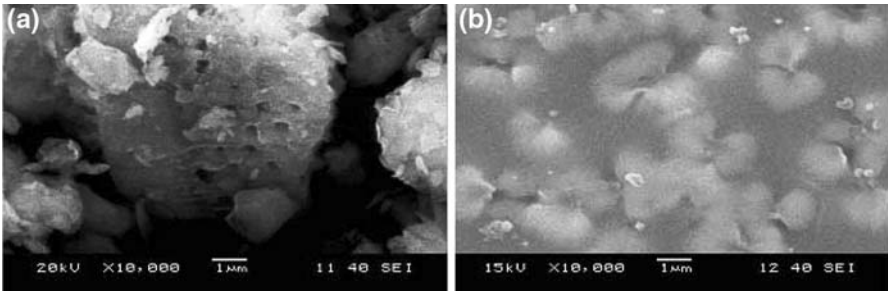

Fig. 4 SEM micrographs of **a** Al-K10 (10,000× magnification) and **b** Al-K10 containing acrylic-based superabsorbent hydrogel composites

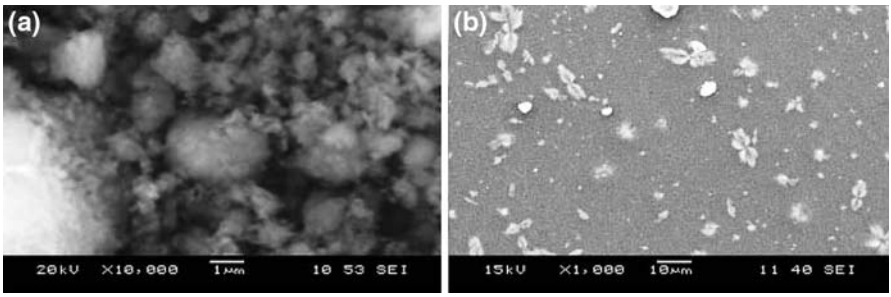

Fig. 5 SEM micrographs of **a** Al-KSF containing acrylic-based superabsorbent hydrogel composites (1,000× magnification) and **b** Al-KSF (10,000× magnification)

FT-IR analysis

The structure of Al-KSF-SA and Al-K10-SA composites was confirmed by FTIR analysis. Table 1 lists the functional groups available in K10, Al-K10-SA, KSF,

Table 1 The characteristic FT-IR data of the samples

IR bands	Samples					
	K10	Al-K10	Al-K10 composite	KSF	Al-KSF	Al-KSF composite
Al_2OH (octahedral layer) (cm^{-1})	3,623	3,622–3,616	3,647	3,620	3,624	3,629
Stretching vibrations of H_2O (cm^{-1})	3,428	3,436	3,395–3,345	3,411–3,389	3,429	3,439–3,363
Stretching vibration of $–CH_2$ (cm^{-1})			2,988–2,881			2,956–2,871
Stretching vibration of C=O (cm^{-1})			1,750			1,722
Bending vibrations of H_2O (cm^{-1})	1,633	1,636	1,682	1,636	1,633	1,621
Asymmetric vibration of R–COOK (cm^{-1})			1,539			1,554
Bending vibration of $–CH_2$ (cm^{-1})			1,463			1,445
Symmetric vibration of R–COOK (cm^{-1})			1,402			1,402
Asymmetric stretching vibrations of SiO_2 tetrahedra (cm^{-1})	1,046	1,041	1,076	1,046	1,041	1,075
Bending vibrations of Al_2OH (cm^{-1})	920	921	915	917	921	914
Stretching vibration of Al^{IV} tetrahedra (cm^{-1})	798	796	800	794	794	806
Bending vibration of Si–O (cm^{-1})	524	528	524	523	526	520
	468	471	469	467	471	482

Al-KSF, and Al-KSF-SA samples. OH stretching vibration of Al-K10 was in the range 3,622–3,647 cm^{-1}. After grafting of SA, this band shifted to 3,647 cm^{-1}. It is interesting to note that OH stretching vibration for Al-KSF was obtained at 3,624 cm^{-1}. However, after fabricating Al-KSF-SA composite, this band slightly shifted to 3,629 cm^{-1}. It can be said that a little interaction generates between OH groups of Al-KSF and SA. Thus, formation of additional network occurs slightly. This means higher swelling ratio for Al-KSF-SA composite. The new absorption bands are appeared at 2,988–2,881 cm^{-1} for Al-K10-SA and 2,956–2,871 cm^{-1} for Al-KSF-SA due to $–CH_2$ stretching vibrations. Bending vibration of $–CH_2$ groups of Al-K10-SA and Al-KSF-SA were located at 1,463 and 1,445 cm^{-1}, respectively. Stretching vibration of C=O group was observed at 1,750 and 1,722 cm^{-1} for Al-K10-SA and Al-KSF-SA, respectively. This new band may be on account of ester formation. The carboxylate groups of the grafted poly(acrylic acid) may react with OH groups on the surface of Al-K10 and Al-KSF-SA leading to ester formation. Asymmetric and symmetric vibrations of R–COOK groups appear 1,539 and 1,402 cm^{-1} for Al-K10-SA and 1,554 and 1,402 cm^{-1} for Al-KSF-SA, respectively. The band around 1,045 cm^{-1} is due to asymmetric stretching vibrations of SiO_2 tetrahedral. After polymerization, stretching vibrations of SiO_2 tetrahedral was shifted to 1,076 and 1,075 cm^{-1} for Al-K10 and Al-KSF based composites, respectively. It indicates the esterification of carboxylic acid with silanol. This mechanism was supported by shifting of the OH stretching vibration of clays and pillared clays. These results may confirm the grafting reaction between pillared clays and the acrylic network through ester formation. A band around 800 cm^{-1} is due to stretching vibration of Al_{IV} tetrahedral, when substitution of Al for Si is low; Al_2OH vibration lies in the 915 ± 950 cm^{-1} range, and absorption at 526–469 cm^{-1} is due to bending of Si–O vibration. These IR characteristic bands of clay were observed and only little shifts were noticeable in pillared clays and the network of pillared clay-based composites from Table 1. The little shifts of these all bands showed that the basic clay layer structure remains unaffected on pillaring and polymerization. These results suggested that the pillaring agents physically entrapped within the PILC structure.

XRD analysis

The change of the interlayer distance can be detected by XRD. The X-ray diffraction patterns of Al-K10, Al-KSF, Al-K10-SA, and Al-KSF-SA are shown in Figs. 6, 7. There is intense diffraction for KSF, K10, Al-KSF, and Al-K10 at $2\theta = 6.50°$ approximately while no diffraction peak appears for Al-K10-SA and Al-KSF-SA suggesting that clay sheets are exfoliated and uniformly dispersed in organic network. These peaks are assigned to the 001 lattice spacing of montmorillonite. The lattice spacing of K10, KSF, Al-K10, and Al-KSF are 14.83 Å at $2\theta = 5.94°$, 12.55 Å at $2\theta = 6.99°$, 17.67 Å at $2\theta = 5.16°$, and 14.15 Å at $2\theta = 6.65°$, respectively. The distance between the layers for Al-K10 and Al-KSF is 2.84 and 1.60 Å, respectively. This shows that the orientation of Al_xO_y (pillaring agent) is different in interlayer of K10 and KSF. 001 lattice spacing of clays were increasing by pillaring. These data supported that clays were pillared by Keggion ion. After polymerization with pillared

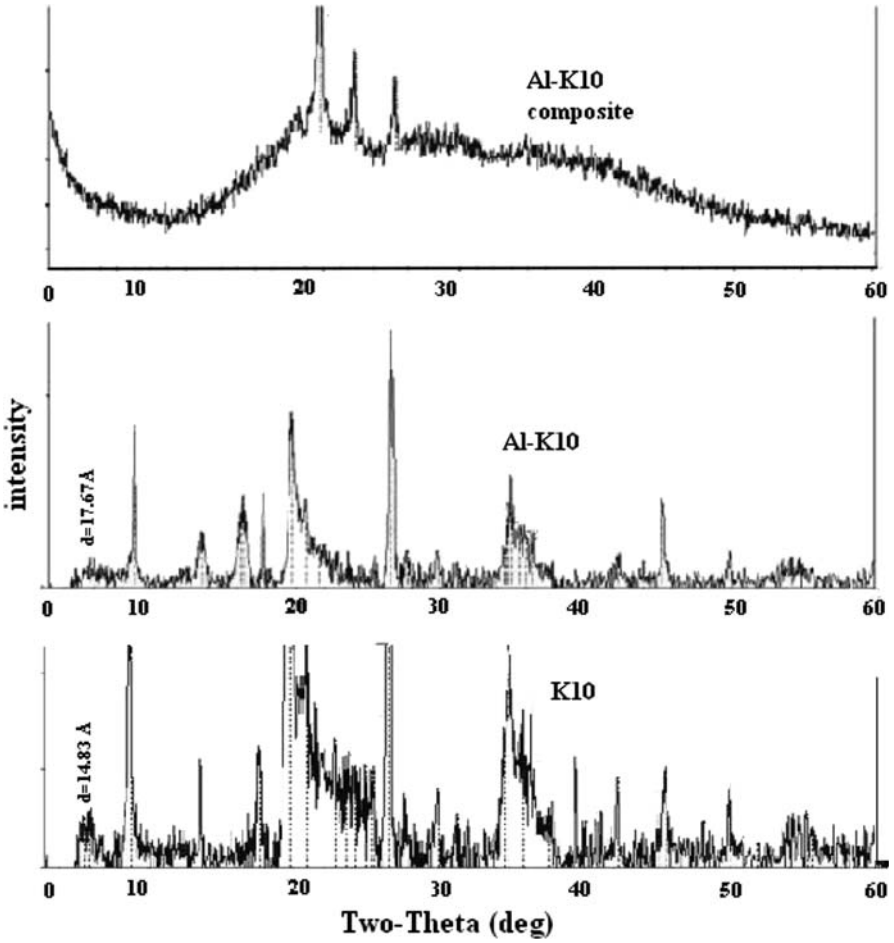

Fig. 6 XRD patterns of K10, Al-K10, and Al-K10-SA composite

clays the diffraction peak corresponding to the montmorillonite is not observed. Pillared clay-based composites presented a low swelling value. It is known that if the increase in the basal space is very high, the forces that keep the layers together are not enough to keep an intercalated structure generating an exfoliated structure. Considering XRD analysis, it may be probable that layers of montmorillonite are dispersed in a continuous polymer matrix as single layers. The XRD patterns of Al-K10 and Al-KSF based composites showed three and two crystal peaks at 2θ of $\sim 20°$ and 30°, respectively. These data support the presence of layers of clays.

Conclusions

This study involved the preparation of pillared clay-based superabsorbent composites. Al-K10 and Al-KSF used as pillared clays. After grafting occurred between

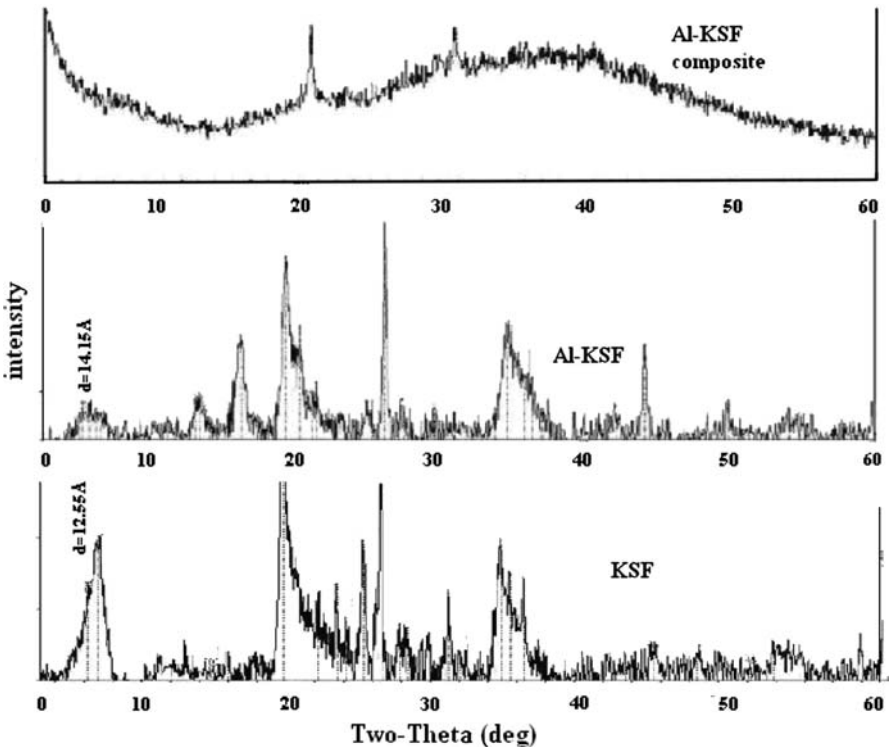

Fig. 7 XRD patterns of KSF, Al-KSF, and Al-KSF-SA composite

pillared clays and the acrylic network, swelling character of composites were revealed out. pH affected swelling character of composites. The swelling behavior of Al-KSF and Al-K10 based superabsorbent films seemed to be pH dependent. It was very essential for new application fields, for example, drug delivery at human system. For both pillared clay-based composite, shrinkage was occurred at low pH values. At basic pH condition, the composites showed swelling behavior. Additionally, reversible swell–shrink properties of Al-KSF and Al-K10 based superabsorbents revealed by using buffer solutions at different pH values. It was beneficial characteristics for pH sensitive systems with controllable swelling ability. The percentages of equilibrium swelling values in distilled water were at about 7900 for Al-KSF SA and at about 5700 for Al-K10 SA. The products were characterized by SEM, FTIR, and XRD. Characterization methods supported the swelling behavior of composites. SEM images indicated that the homogeny dispersion of pillared clay on Al-KSF based composite was lower than Al-K10 based composite and the pores were observed clearly from the morphology of Al-K10. From FTIR analysis, IR characteristic bands of clay were observed in pillared clays and the network of pillared clay-based composites. It was understood that the clay layer structure remain unaffected by polymerization. The shifts seen of stretching vibrations of SiO_2 tetrahedron and OH bands supported ester formation between acrylic network and pillared clay.

The XRD results indicated that the peaks assigned to the 001 lattice spacing of montmorillonite were not observed and layers of montmorillonite are completely dispersed in a continuous polymer matrix as single layers thus pillared clay-based composites presented a low swelling value. It supported that the crosslinking was higher and swelling ratio of Al-K10 based composite is lower than Al-KSF based composite. It can be concluded that these properties of superabsorbents would be valuable for many application field in which hydrogels were used. Pillared clays could not protect the layered silicate structure upon fabricating composites with graft copolymerization of acrylic acid.

Acknowledgments The authors thank the scholarship for Zehra Bekçi Molu supported by TÜBİTAK MÜNİR BİRSEL Foundation/Turkey. The authors are also grateful to Research Foundation of Dokuz Eylül University (Project No: 2007.KB.FEN.028) for financial support.

References

1. Li A, Zhang J, Wang A (2005) Synthesis, characterization and water absorbency properties of poly(acrylicacid)/sodium humate superabsorbent composite. Polym Adv Technol 16:675–680
2. Yao KJ, Zhou WJ (1994) Synthesis and water absorbency of the copolymer of acrylamide with anionic monomers. J Appl Polym Sci 53:1533–1538
3. Zhou WJ, Yao KJ, Kurth MJ (1996) Synthesis and swelling properties of the copolymer of acrylamide with anionic monomers. J Appl Polym Sci 62:911–915
4. Tsubakimoto T, Shimomura T, Kobabyashi H (1987) Japanese Patent 62,149-335
5. Miura Y, Hirano K, Nate T, Kambayashi T, Ohtsuka M, Nagai T (1991) European Patent 440: 256
6. Tanaka H, Kambayashi T, Sugiyama Y, Nagai T, Nagata K, Kubota K, Hirano K (1992) European Patent 501:482
7. Walker CO (1987) US Patent 4: 664 816
8. Colombo P (1993) Swelling-controlled release in hydrogel matrices for oral route. Adv Drug Deliv Rev 11:37–57
9. Dong LC, Hoffman AS (1991) A novel approach for preparation of pH-sensitive hydrogels for enteric drug delivery. J Control Release 15:141–152
10. Zhang J, Li A, Wang AQ (2005) Study on superabsorbent composite. V. Synthesis, swelling behaviors and application of poly(acrylic acid-co-acrylamide)/sodium humate/attapulgite superabsorbent composite. Polym Adv Technol 16:813–820
11. Wu JH, Wei YL, Lin SB (2003) Study on starch-graft-acrylamide/mineral powder superabsorbent composite. Polymer 44:6513–6520
12. Lee WF, Yang LG (2004) Superabsorbent polymeric materials. XII. Effect of montmorillonite on water absorbency for poly(sodium acrylate) and montmorillonite nanocomposite superabsorbents. J Appl Polym Sci 92:3422–3429
13. Kabiri K, Zohuriaan-Mehr MJ (2004) Porous superabsorbent hydrogel composites: synthesis, morphology and swelling rate. Macromol Mater Eng 289:653–661
14. Su XF, Zhang G, Xu K, Wang J, Song C, Wang P (2008) The effect of MMT/modified MMT on the structure and performance of the superabsorbent composite. Polym Bull 60:69–78
15. Li A, Wang AQ, Chen JM (2004) Studies on poly(acrylic acid)/attapulgite superabsorbent composite. I. Synthesis and characterization. J Appl Polym Sci 92:1596–1603
16. Wang WB, Zheng YA, Wang AQ (2008) Syntheses and properties of superabsorbent composites based on natural guar gum and attapulgite. Polym Adv Technol 19:1852–1859
17. Lin J, Wu J, Yang Z, Pu M (2001) Synthesis and properties of poly(acrylic acid)/mica superabsorbent nanocomposite. Macromol Rapid Commun 22:422–424
18. Wu J, Lin J, Zhou M, Wei C (2000) Synthesis and properties of starch-graft-polyacrylamide/clay superabsorbent composite. Macromol Rapid Commun 21:1032–1034

19. Zhang Y, Fan L, Zhao P, Zhang L, Chen H (2008) Preparation of nanocomposite superabsorbents based on hydrotalcite and poly (acrylic-co-acrylamide) by inverse suspension polymerization. Comp Interfaces 15(7–9):747–757
20. Lothenbach B, Furrer G, Schulin R (1997) Immobilisation of heavy metals by polynuclear aluminium and montmorillonite compounds. Environ Sci Technol 31:1452–1462
21. Ding Z, Zhu HY, Greenfield PF, Lu GQ (2001) Characterization of pore structure and coordination of titanium in TiO_2 and SiO_2-TiO_2 sol-pillared clays. Colloid Interface Sci 238:267–272
22. Ding Z, Kloprogge JT, Frost R, Zhu LH (2001) Porous clays and pillared clays-based catalysts. Part 2: a review of the catalytic and molecular sieve applications. J Porous Mater 8:273–293
23. Wan T, Lin J, Li X, Xiao W (2008) Preparation of epoxy-silica-acrylate hybrid coatings. Polym Bull 59:749–758
24. Zhang Y, Fan L, Cheng L, Zhang L, Chen H (2009) Preparation and morphology of high-performance exfoliated poly (sodium acrylate)/hydrotalcite nanocomposite superabsorbents. Polym Eng Sci 49:264–271
25. El-Hamshary H (2007) Synthesis and water sorption studies of pH sensitive poly(acrylamide-co-itaconic acid) hydrogels. Eur Polym J 43:4830–4838
26. Kabiri K, Zohuriaan Mehr MJ (2003) Superabsorbent hydrogel composites. Polym Adv Technol 14:438–444
27. Seki Y, Torgürsül A, Yurdakoc K (2007) Preparation and characterization of poly(acrylic acid)-iron rich smectite superabsorbent composites. Polym Adv Technol 18:477–482
28. Zhang J, Wang A (2007) Study on superabsorbent composites. IX: synthesis, characterization and swelling behaviors of polyacrylamide/clay composites based on various clays. React Funct Polym 67(8):737–745